Urol Res (2005) 33: 31–38
DOI 10.1007/s00240-004-0434-6

ORIGINAL PAPER

Katsuhito Miyazawa · Koji Suzuki · Ryosuke Ikeda
Manabu T Moriyama · Yoshimichi Ueda
Shogo Katsuda

Apoptosis and its related genes in renal epithelial cells of the stone-forming rat

Received: 7 July 2003 / Accepted: 26 April 2004 / Published online: 3 July 2004

Abstract Experimental hyperoxaluria and calcium oxalate (CaOx) crystals are associated with renal epithelial injury and cell death. A recent study has demonstrated an oxalate-induced increase in cellular apoptosis in vitro, and speculates that this phenomenon may contribute to stone formation. We investigated the incidence of apoptotic cells and the expression of apoptosis related genes in the kidneys of stone-forming rats. Male Wistar rats were administrated ethylene glycol in drinking water and force fed with1α-OH-D_3. Apoptosis was detected as a ladder of fragmented DNA in agarose gels of electrophoresed genomic DNA. Apoptotic cells were localized by the terminal deoxynucleotidyl transferase-mediated dUTP-biotin nick end labeling (TUNEL) method. The expression of apoptosis-related genes was analyzed by both reverse transcription polymerase chain reaction (RT-PCR) and immunohistochemistry. While no labeling was detected in the controls or on the first day of administration by the TUNEL method, labeling began to be detected in the renal tubular epithelium of the outer medulla at day 3, and the number of labeled cells increased progressively during the observation period. A ladder of DNA fragments was demonstrated in the kidneys of rats after 2 weeks. Immunohistochemical studies revealed the expression of Fas ligand (Fas L), Bax and interleukin-1 β converting enzyme (ICE) in the renal tubular epithelium of the descending limb of loop of Henle and the distal convoluted tubules. mRNA of the ICE, c-*myc*, *p53* and Fas L genes was also upregulated in the kidneys of the stone-forming rats.

K. Miyazawa (✉) · K. Suzuki · R. Ikeda · M. T. Moriyama
Department of Urology, Kanazawa Medial University,
Uchinada, Ishikawa, 920-0293 Japan,
E-mail: miyazawa@kanazawa-med.ac.jp
Tel.: +81-76-286-2211
Fax: +81-76-286-5516

Y. Ueda · S. Katsuda
Department of Pathology, Kanazawa Medial University,
Uchinada, Ishikawa, Japan

Keywords Calcium oxalate · Crystal · Urolithiasis · Apoptosis · Stone-forming rat

Introduction

The first step in urolithiasis is considered to take place in the lumen of the renal tubules, after which the renal tubular cells participate in the development of stone [1, 2]. This relationship between the crystals and renal tubular cells, the so-called crystal-cell interaction, is considered to play an important role in the early stage of crystal formation. The exact molecular mechanisms involved at the crystal-tissue interface, specific crystal-molecular interactions and the mechanism of growth of crystal precipitates, have not been well elucidated, however, there is evidence that tubular damage occurs in both clinical and experimental stone disease [3, 4, 5]. Tubular damage increases the incidence of plaque and stones in experimental animals [6], disrupts renal epithelial polarity in vitro, promoting crystal binding [7], and the addition of membrane fractions from renal tubular cells promotes the growth of calcium oxalate (CaOx) crystals in artificial urine [8]. These considerations suggest that hyperoxaluria and crystal mediated cellular response play a role in the pathogenesis of urolithiasis.

Programmed cell death, which is involved in vital defense and the maintenance of homeostasis, is now widely known as apoptosis and has been reported to be implicated in various diseases [9]. The participation of apoptosis in various renal diseases, such as progressive crescentic glomerulonephritis, glomerular sclerosis, ischemic tubular necrosis, drug induced tubular damage and polycystic kidney disease [10], has been reported, and recent studies provide evidence for oxalate induced increases in cellular apoptosis in renal epithelial cell lines and rabbit renal tubular cells, and speculate that this phenomenon may contribute to stone formation [11, 12, 13].

We examined the incidence and localization of apoptosis and the expression of apoptosis related genes,

at both the mRNA and protein levels, in the rat model of hyperoxaluria, with subsequent CaOx crystal formation.

Materials and methods

The induction of hyperoxaluria and formation of CaOx crystals in the rat kidney, and tissue preparations

CaOx crystals were induced by the administration of 0.5% ethylene glycol (EG) in the drinking water and forced feeding of 0.5 μg 1α-OH-D_3 (Chugai, Tokyo) every other day through a gastric tube to 7-week old Wistar rats (200–250 g) [14]. Both kidneys were excised on day 1 (G-1), day 3 (G-2), day 5 (G-3), day 7 (G-4), week 2 (G-5), week 3 (G-6) and week 4 (G-7) during the administration of EG and 1α-OH-D_3. There were five rats per group. Kidneys were also excised from five normal, control rats. The right kidney was divided into four parts, each uniformly containing parts from the renal cortex to the medulla, which were immediately frozen in liquid nitrogen and stored at −80°C until use. The left kidney was fixed in 4% paraformaldehyde at 4°C for 8 h, dehydrated by graded alcohol series and then embedded in paraffin.

Terminal deoxynucleotidyl transferase mediated dUTP-biotin nick end labeling

The DNA 3′-terminal was labeled by the terminal deoxynucleotidyl transferase mediated dUTP-biotin nick end labeling (TUNEL) method [15] using an in situ apoptosis detection kit (S7100-KIT, Oncor, Gaithersburg, Md.) on 3 μm thick 4% paraformaldehyde-fixed, paraffin-embedded sections according to the manufacture's instructions. Briefly, after deparaffinization, protein was digested by proteinase K (0.1 mg/ml) at 37°C for 15 min, and endogenous peroxidase was inactivated by 3% H_2O_2/methanol for 10 min. The section was incubated with deoxynucleotidyl transferase for 1 h at 37°C. After termination of the reaction, the tissue was incubated with peroxidase labeled antidigoxigenin antibody for 30 min at room temperature. Color was developed using 0.02% 3,3′diaminobenzidine tetrahydrochloride. As a positive control, paraffin-embedded sections of human tonsils were used. Two pathologist examined the slides in order to avoid bias. The number of positive cells (mean ± standard deviation) was counted in five representative fields using a 20× objective lens. The fields for the quantification of positive cells were selected in the renal medulla where crystals appeared, and TUNEL positive cells from the epithelial lining of the tubules.

Agarose gel electrophoresis of DNA

Genomic DNA was extracted by the proteinase K-sodium dodecyl sulfate digestion method from frozen tissues [16]. The extracted DNA (10 μg) was dissolved in TE solution (100 mM Tris-HCl, pH 8.0, 1 mM EDTA), and subjected to electrophoresis in a 2% agarose gel (Agarose 21, Nippon Gene, Toyama). The gel was stained with ethidium bromide and observed under ultraviolet light (NLMS-20E, Funakoshi, Tokyo).

Histological and immunohistochemical staining

Continuous thin sections, 4 μm in thickness, were prepared from the 4% paraformaldehyde-fixed, paraffin-embedded samples. Von Kossa staining was used to determine the location of CaOx. The expression of apoptosis-related genes, such as Fas ligand (Fas L), Bax, bcl-2 and interleukin-1 β converting enzyme (ICE), were detected by the streptavidin-biotin complex method. Endogenous peroxidase was inactivated by 3% H_2O_2 and non-specific reactions were blocked by normal serum before the incubation with anti-Fas L monoclonal antibody (Transduction Laboratories, Ky., 0.25 μg/ml), anti-Bax monoclonal antibody (Immunotech, Marseille, supplied in the working concentration and directly applied), anti-human bcl-2 oncoprotein (Dako, Copenhagen, 0.5 μg/ml) or anti-ICE polyclonal antibody (M-19, Santa Cruz, Calif., 1 μg/ml). For the immunostaining of Bax, signals were amplified by the catalyzed signal amplification system (Dako, Copenhagen).

Reverse transcription-polymerase chain reaction analysis

Total RNA was extracted by the acid guanidium thiocyanate-phenol-chloroform method [17]. The poly $(A)^+$ RNA was purified from the total RNA using oligo (dT)-latex particles (Oligotex-dT30: Roche, Tokyo) [18]. The cDNA was synthesized using reverse transcriptase (Superscript RII: Gibco BRL, Gaithersburg, Md.) at 37°C for 30 min. Expression of the ICE, *c-myc, bcl-2* and *p53* genes at the messenger level was analyzed using an MPCR kit for rat apoptosis genes-I (MBI, San Francisco, Calif.) according to the manufacture's instructions. The expression of the *Fas L* gene was examined using the sense primer, 5′-TCTGGTTGGAATGGGGTTAG-3′, and anti-sense primer, 5′ATTAGCACCAGATCCCCAGG-3′, by PCR (PTC-100, MJ Research, Mass.) with 33 cycles with denaturation at 94°C for 0.5 min, annealing at 60°C for 2 min and extension at 72°C for 3 min. The PCR product was electrophoresed on a 2% agarose gel, stained with ethidium bromide and observed under ultraviolet light (NLMS-20E, Funakoshi, Tokyo) with the positive control, supplied from the company (MBI) or the PCR product with normal rat lung for Fas L, as a standard to analyze the expression of each gene. As an internal standard, we prepared the primers against glyceraldehyde-3-phosphate dehydrogenase (G3PDH), sense primer, 5′-TCAAGGTCGGTGTCAACGGATTTGGC-3′, and anti-sense primer, 5′-CATCTAGGCCATGAGGTCCACCAC-3′ and performed PCR under

the same conditions. As a negative control, PCR was performed using non-reverse transcribed mRNA.

Results

Formation of CaOx crystal

CaOx crystals were not observed in the kidneys of the control group or day 1 rats. At day 3 of the administration of EG and 1α-OH- D_3, CaOx crystals began to be detected within the lumen and inside of cells of the renal tubules of the descending limb of the loop of Henle and the distal convoluted tubules. Crystal formation increased with the duration of EG administration, and spread to the lumens of the renal papillary collecting ducts and the proximal convoluted tubules. The lumens of some renal tubules became distended (Fig. 1).

Analysis of apoptosis

TUNEL method

Labeling due to the TUNEL method was hardly detected in the control and day 1 groups. From day 3, labeling was detected in the renal tubular epithelium of the descending limb of the loop of Henle, where CaOx began to precipitate. No significant positive cells were detected in the renal glomerulus or renal interstitium. Some TUNEL-labeled cells were detached from the tubules. The number of TUNEL-positive cells increased with time and spread to the distal tubular epithelium (Fig. 2). The number of apoptotic cells increased significantly from 6.2 ± 4.2 at day 3 to 41.4 ± 6.4 at 4 weeks/five microscope fields of ×20 ($P < 0.0001$, Kruskal-Wallis test) during EG and 1α-OH-D_3 administration (Fig. 3).

Electrophoresis of DNA

DNA ladder formation with a unit of 180 bp was detected by the electrophoresis of DNA extracted from rat kidneys at week 4. No ladder formation was detected in the DNA prepared from the control rats (Fig. 4).

Expression of apoptosis related genes

Immunohistochemical study

The expression of ICE (caspase 1), Bax, bcl-2 and Fas L were studied by immunohistochemistry. ICE (caspase 1)

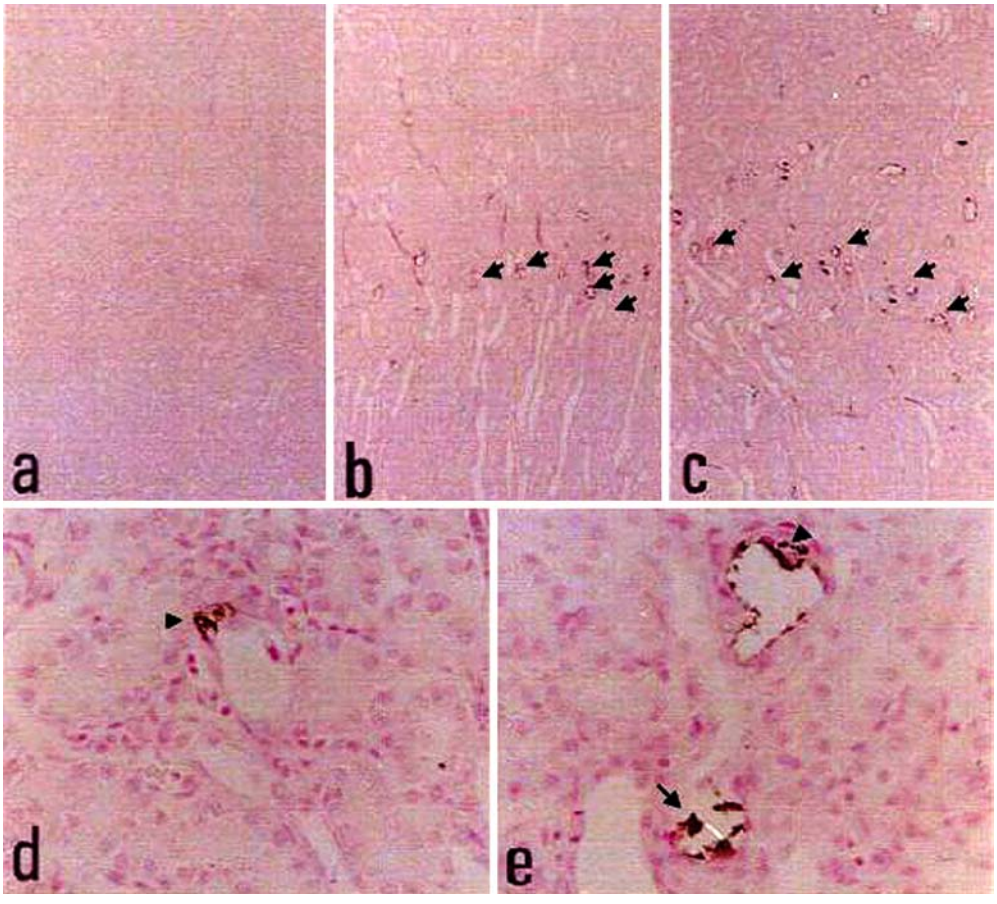

Fig. 1 Distribution of crystals formed in rats by the administration of ethylene glycol and 1α-OH-D_3. **a** No crystals are seen in the kidney of the control rat. **b** A small amount of crystal precipitation (*arrows*) is seen in the outer medulla of the kidney 5 days after the induction of crystal formation. **c** Abundant crystal formation (*arrows*) is seen at the same site at 4 weeks after the induction of crystal formation. **d** High power section of **b**. Crystals are seen inside of tubular epithelial cells (*arrowhead*). **e** High power section of **c**. Crystals are seen both in the lumen (*arrows*) and inside of tubular epithelial cells (*arrowhead*). Hyperchromatic, aggregated nuclei appears to surround a crystalline concretion. Von Kossa stain, **a**–**c** ×25, **d**, **e** ×250

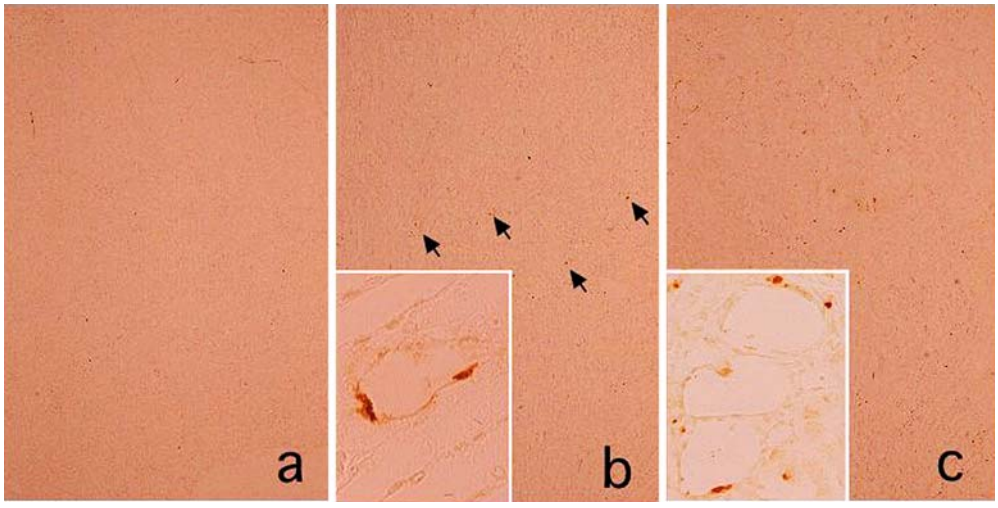

Fig. 2 Detection of apoptosis by the TUNEL method in ethylene glycol and 1α-OH-D_3-administrated rat kidney. **a** Positive labeling was hardly detected in the control kidney. **b** Labeling was detected in the outer medulla at 5 days after the induction of crystal formation. **c** Labeling had increased and spread at 4 weeks after the induction of crystal formation. *Inset* of **b** and **c**: label was observed in the nuclei of the renal tubular epithelium of the descending limb of the loop of Henle and the distal convoluted tubules at 5 days after and 4 weeks after the induction of crystal formation. **a**, **b**, **c** ×25, *inset* of **b**, **c** ×250

was first detected in the epithelium of the distal convoluted tubules on day 5. With the course of EG and 1α-OH-D_3 administration, distal tubular epithelium showed increased positive reactions for ICE. Bax was also localized in the epithelium of the distal convoluted tubules on day 5. With the course of EG and 1α-OH-D_3 administration, distal tubular epithelia also showed strong positive reactions for Bax. Bcl-2 was localized in the epithelium of the distal convoluted tubules of both the controls and rats with crystal formation. Fas L was localized in the epithelium of the distal convoluted tubules on day 5 and week 4 (Fig. 5).

RT-PCR

The expression of the G3PDH gene was detected in the kidneys of both the controls and rats with crystal

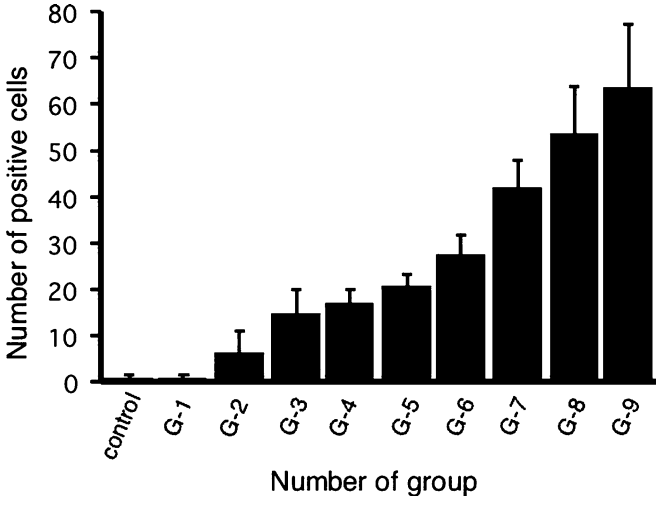

Fig. 3 Numbers of TUNEL-labeled renal tubular epithelial cells in ethylene glycol and 1α-OH-D_3-administrated rat kidney. Values are mean ± standard deviation/five microscope fields of ×20, 0.8 ± 0.8; *G-1* (day 1), 0.6 ± 0.9; *G-2* (day 3), 6.2 ± 4.2; *G-3* (day 5), 14.6 ± 3.4; *G-4* (day 7), 16.6 ± 3.4; *G-5* (week 2), 20.4 ± 3.2; *G-6* (week 3), 27.4 ± 4.5; *G-7* (week 4), 41.4 ± 6.4. ($P < 0.0001$, Kruskal-Wallis test)

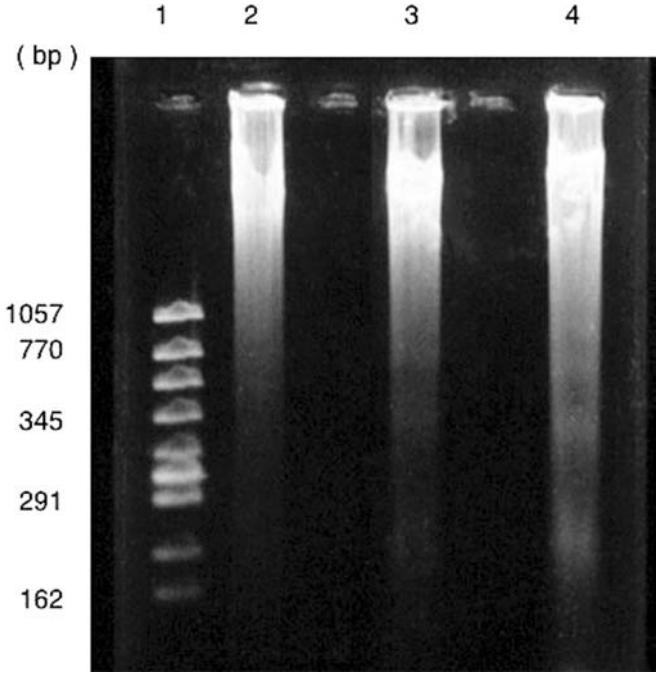

Fig. 4 DNA fragmentation seen by electrophoresis in ethylene glycol and 1α-OH-D_3-administrated rat kidney; *lane 1*, size marker; *lane 2*, control rat; *lane 3*, 5 days after the induction of crystal formation; *lane 4*, 4 weeks after the induction of crystal formation. DNA ladder formation with units of 180 bp is observed in *lane 4*. In *lane 2*, intact DNA is seen without DNA ladder formation

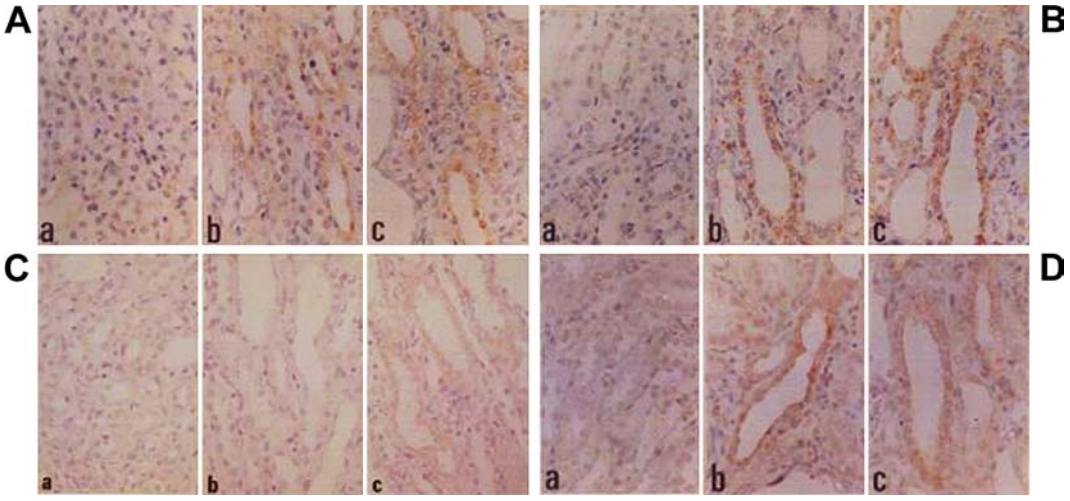

Fig. 5 **A** Expression of ICE in the kidneys of rats with crystal formation. *a* ICE is not expressed in the kidneys of the control rat. *b*, *c* ICE was detected in the distal convoluted tubular cells on day 5 and week 4. *a*, *b*, *c* ×250. **B** Expression of Bax in the kidneys of rats with crystal formation. *a* Bax is not expressed in the kidney of the control rat. *b*, *c* Expression of Bax is seen in the distal convoluted tubular cells on day 5 and week 4. *a*, *b*, *c* ×250. **C** Expression of bcl-2 in the kidney. *a*, *b*, *c* Bcl-2 was weakly localized in distal convoluted tubular cells of the control rats and rats with crystal formation on day 5 and week 4. *a*, *b*, *c* ×250. **D** Expression of Fas L in the kidney of rats with crystal formation. *a* Fas L is not expressed in the kidney of the control rat. *b*, *c* Fas L was localized in distal convoluted tubular cells on day 5 and week 4. *a*, *b*, *c* ×250

formation, and expression of Fas L mRNA is detected in the kidneys of the rats with crystal formation, but not in those of the control rats (Fig. 6). The expression of ICE, *c-myc* and *p53* genes was detected in the kidneys of the rats with crystal formation, but not in those of the control rats. The expression of the *Bcl-2* gene was detected in the kidneys of the controls as well as rats with crystal formation (Fig. 7).

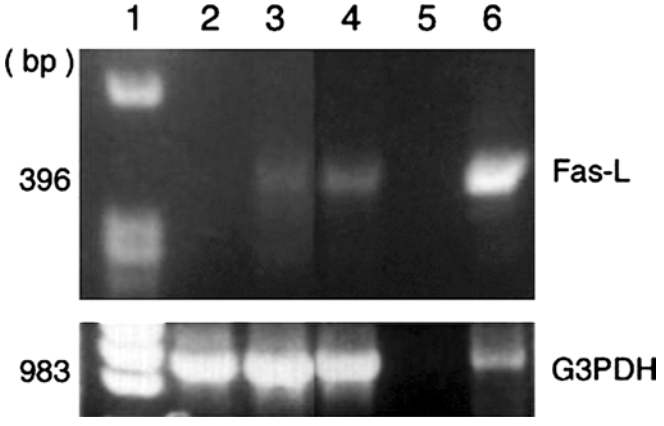

Fig. 6 Expression of *Fas L* by RT-PCR in rat kidneys with crystal formation. *Lane 1*, size marker; *lane 2*, control rat; *lane 3*, day 5; *lane 4*, week 4; *lane 5*, negative control; *lane 6*, positive control (rat lung). Expression of Fas L mRNA was detected in the kidneys of the rats with crystal formation, but not in those of the control rats. G3PDH mRNA was expressed in the kidneys of both the control rats and the rats with crystal formation

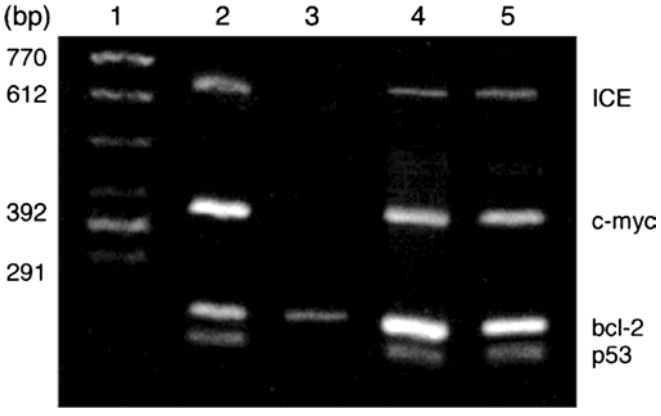

Fig. 7 Expression of ICE, *c-myc*, *Bcl-2* and *p53* by RT-PCR. *Lane 1*, size marker; *lane 2*, positive control; *lane 3*, control rat; *lane 4*, day 5; *lane 5*, week 4. The *Bcl-2* gene was expressed in the kidneys of both control rats and rats with crystal formation. Expression of ICE, *c-myc* and *p53* genes was observed in rat kidneys with crystal formation (day 5, and week 4), but not in control kidneys

Discussion

The issue of where urolithiasis begins is controversial. Recent findings that crystals are retained in the kidney after rapid adhesion to the tubular surface of the renal tubular cells, and that the renal tubular cells endocytose the CaOx crystals [19] support the view that stone formation begins in the lumen of renal tubules [1]. On the other hand, light and electron microscopic observations of rats after the oral administration of EG and ammonium chloride reported by Boeve et al. [2] support the view that stone formation begins in renal tubular cells. In either case, it is difficult to explain the pathophysiology of urolithiasis by the crystallization process alone, and a close relationship between the crystals and renal tubular cells has been suggested [20, 21, 22, 23, 24, 25]. Hammes et al. [26] reported that CaOx monohydrate crystals activate specific gene expression in the renal epithelial cells and contribute to the progression of interstitial fibrosis, indicating that crystals may regulate

the expression of a repertoire of important genes. Oxalate, the most common constituent of urolithiasis, is excreted primarily by the kidney. There are a variety of transport systems in the proximal and distal tubular cells to remove oxalate [27, 28]. Oxalate accumulates intracellularly within renal epithelial cells during the transcellular flux [29]. This accumulation has been considered benign, however, recent studies have revealed that oxalate acts as a mitogen at low concentrations [30] and as a toxin at high concentrations [31] in LLC-PK_1 cells.

Apoptosis has recently been found to play a pivotal physiological role in the elimination of embryonal cells not required in later development, cells that have not differentiated normally, senescent cells, and cells that have been damaged [32]. Apoptotic changes include exposure of annexin binding phosphatidylserine to the cell surface as well as morphological changes [33, 34, 35]. Clusters of negatively charged head groups of phosphatidylserine attract calcium and can act as sites for the attachment of calcific crystals to the cell surfaces [36]. Such clusters on surfaces of apoptotic bodies and membranous cellular degeneration products can promote the nucleation of calcific salts [8, 37]. Thus apoptosis is one of mechanisms of crystal attachment to epithelial cells following injury, and may play an important role in nephrolithiasis [38].

We investigated the incidence and distribution of apoptosis and the expression of apoptosis related genes to clarify whether cell injury and death are due to apoptotic activity using a standard method of inducing hyperoxaluria and CaOx crystalluria and intrarenal CaOx crystal deposition. While TUNEL-labeled cells were hardly detected in the control kidneys, positive cells were detected in the epithelium of the descending limb of the loop of Henle and the distal convoluted tubules at an early phase of the administration. These increased with time and spread to the epithelia of the proximal convoluted tubules in the late phase. These findings suggest that cell injury caused by oxalate and subsequent crystallization may switch on apoptosis inducing genes in the renal epithelial cells. Moreover, it is interesting to note that the macromolecular stone matrix, an important constituent of kidney stone, such as heparan sulfate, bikunin, Tamm-Horsfall mucoprotein, osteopontin and urinary prothrombin fragment-1, distributes in the same portion of nephron [39, 40]. It is reasonable to consider that these sites are closely related to stone formation.

There are a few reports on apoptosis and oxalate toxicity in renal epithelial cells [11, 12, 13], however apoptosis and the expression of its related genes in a stone forming rat model have not been described. EG feeding is a standard method for the rat model, however, renal damage following EG feeding is a result not only of oxalate but also of other metabolites. The evaluation of other models, such as oxalate or glycolate, is needed to demonstrate the direct relationship between hyperoxaluria and apoptosis. Since the study of the relationship between apoptosis and urolithiasis has just began, and the exact role of apoptosis in the renal epithelial cells with oxalate and CaOx crystals remains unknown, further studies are needed to confirm whether apoptosis in the renal cellular epithelium assists in membrane associated nucleation and the aggregation of CaOx.

An apoptosis suppressor gene, *Bcl-2*, and apoptosis inducing genes, Fas L, ICE, *p53*, *c-myc* and *Bax*, were upregulated in renal tubular cells during crystal formation. High expression of Bcl-2 was observed in mesenchymal and epithelial structures in the developing kidney. With maturation, weak expression was shown in glomerular epithelial cells as well as tubules, indicating activity to suppress apoptosis in these layers [10]. Bax, one of the Bcl-2 family, forms a heterodimer with Bcl-2. One Bax molecule forms a heterodimer with Bcl-2. It also forms a homodimer with another Bax. Apoptosis is accelerated when the amount of Bax-Bax homodimer exceeds that of the Bcl-2-Bax heterodimer [41]. By RT-PCR, *Bcl-2* expression was detected in the kidneys of both the control rats and the rats with crystal formation. Bax was demonstrated at the protein level only in rats with crystal formation, indicating that it may be involved in the induction of apoptosis in the kidneys of crystal-forming rats. The presence of two pathways for apoptosis, p53-dependent and p53-independent, has been reported [42]. The promoter of the Bax gene is known to have four p53-binding motifs, and the expression of the *Bax* gene is upregulated by p53 [43]. The present findings on the expression of p53 at the messenger level are consistent with the involvement of a p53 dependent pathway. While Hermeking and Eick [44] reported p53-dependent apoptosis by c-myc, Thulasi et al. [45] reported that apoptosis is induced even when c-myc expression is low. c-myc-induced apoptosis was recently shown to require an interaction on the cell surface between CD95 (also termed Fas or APO-1) and its ligand [46]. Fas antigen is a cell surface protein that mediates apoptosis, and Fas mRNA was identified in the renal cells and whole kidney tissue [47]. Fas-L transmits the signal for apoptosis via the Fas receptor [48]. The specific ICE inhibitors, such as crmA product and acetyl Tyr-Val-Ala-Asp-chloromethylketone, inhibit Fas-induced apoptosis. The ICE family has been suggested to be involved in the transmission of the apoptosis signal mediated by Fas [49, 50]. In the present study, the expression of Bax and ICE were seen in both crystals precipitated in tubular epithelium and crystals lacking tubular epithelium, while the expression of Fas L was detected only in crystals precipitated in tubular epithelium. These findings show that apoptosis induced in the rat kidney with crystal formation might have been induced in at least two different ways, p53 dependent and Fas/Fas L mediated.

Conclusions

In the hyperoxaluric, subsequently stone-forming, rat kidney caused by the administration of EG and 1α-OH-D_3, apoptosis was detected in the renal epithelial cells,

especially in those of the descending limb of the loop of Henle, and in the distal convoluted tubules. RT-PCR and immunohistochemical analyses revealed upregulation of Fas-L, ICE, Bax, c-myc and p53. These findings indicate that renal epithelial injury in the stone-forming rat model following EG and 1α-OH-D_3 feeding may induce the expression of these apoptosis-related genes, and different pathways in the stone-forming rat model may induce apoptosis

Acknowledgement This work was supported in the part by Grant in Aid for Science Research C-16591627 from the Ministry of Education, Science, Sport and Culture in Japan.

References

1. Lieske JC, Swift H, Martin T, Patterson B, Toback FG (1994) Renal epithelial cells rapidly bind and internalize calcium oxalate monohydrate crystals. Proc Natl Acad Sci U S A 91: 6987
2. Boeve ER, Ketelaars GAM, Vermeiji M, Cao LC, Schroder FH, De Bruijn WC (1993) An ultrastructural study of experimentally induced microliths in rat proximal and distal tubules. J Urol 149: 893
3. Baggio B, Gambaro G, Ossi E, Favaro F, Borsatti A (1983) Increased urinary excretion of renal enzymes in idiopathic calcium oxalate nephrolithiasis. J Urol 129: 1161
4. Khan SR, Hackett RL (1993) Hyperoxaluria, enzymuria and nephrolithiasis. Contrib Nephrol 101: 190
5. Khan SR, Shevock PN, Hackett RL (1992) Acute hyperoxaluria, renal injury and calcium oxalate urolithiasis. J Urol 147: 226
6. Sigmon D, Kumar S, Carpenter B, Miller T, Menon M, Scheid C (1991) Oxalate transport in renal tubular cells from normal and stone-forming animals. Am J Kidney Dis 17: 376
7. Riese RJ, Mandel NS, Wiessner JH, Mandel GS, Becker CG, Kleiman JG (1992) Cell polarity and calcium oxalate crystal adherence to cultured collecting duct cell. Am J Physiol 262: F177
8. Khan SR, Shevock PN, Hackett RL (1990) Membrane associated crystallization of calcium oxalate in vitro. Calcif Tissue Res 46: 116
9. Thompson CB (1995) Apoptosis in the pathogenesis and treatment of disease. Science 267: 1456
10. Savill J (1994) Apoptosis and the kidney. J Am Soc Nephrol 5: 12
11. Khan SR, Byer KJ, Thamilselvan S, Hackett RL, McCormack WT, Benson NA, Vaughn KL, Erdos GY (1999) Crystal-cell interaction and apoptosis in oxalate-associated injury of renal epithelial cells. J Am Soc Nephrol 10: S457
12. Miller C, Kennington L, Cooney R, Kohjimoto Y, Cao LC, Honeyman T, Pullman J, Jonassen J, Scheide C (2000) Oxalate toxicity in renal epithelial cells: characteristics of apoptosis and necrosis. Toxicol Appl Pharm 162: 132
13. Sarica K, Yagci F, Bakir K, Erbagci A, Erthurhan S, Ucak R (2001) Renal tubular injury induced by hyperoxaluria: evaluation of apoptotic changes. Urol Res 29: 34
14. Okada Y, Kawamura J, Kuo YJ, Yoshida O (1984) Experimental model for calcium oxalate urolithiasis. In: Ryall RL, Brockis JG, Marshall V, Finlayson B (eds) Urinary stone. Churchill Livingstone, New York, p 378
15. Wijsman JH, Jonker RR, Keijzer R (1993) A new method to detect apoptosis in paraffin sections: in situ end-labeling of fragmented DNA. J Histochem Cytochem 41: 7
16. Sambrook J, Fritsch EF, Maniatis T (1989) Isolation of high-molecular-weight DNA from mammalian cells. In: Sambrook J, Fritsch EF, Maniatis (eds) Molecular cloning: a laboratory manual, 2nd edn. Cold Spring Harbor, New York, p 9.14
17. Chomczynski P, Sacchi N (1987) Single-step method of RNA isolation by acid guanidium thiocyanate-phenol-chloroform extraction. Anal Biochem 162: 156
18. Kuribayashi K, Hikata M, Hiraoka O, Miyamoto C, Furuichi Y (1988) A rapid and efficient purification of poly (A)-mRNA by oligo $(dT)^{30}$-latex. Nucleic Acids Res Symp Ser 19: 61
19. Lieske JC, Margaret M, Walsh-Reitz, Toback FG (1992) Calcium oxalate monohydrate crystals are endocytosed by renal epithelial cells and induce proliferation. Amer J Physiol 262: F622
20. Gambaro G, Baggio B (1992) Idiopathic calcium oxalate nephrolithiasis: a cellular disease. Scanning Microsc 6: 247
21. Hackett RL, Shevock PN, Khan SR (1990) Cell injury associated calcium oxalate crystalluria. J Urol 144: 1535
22. Khan SR, Hackett RL (1991) Retention of calcium oxalate crystals in renal tubules. Scanning Microsc 5: 707
23. Lieske CL, Spargo BH, Toback FG (1992) Endocytosis of calcium oxalate crystals and proliferation of renal tubular epithelial cells in a patient with type 1 primary hyperoxaluria. J Urol 148: 1517
24. Mandel N (1994) Crystal-membrane interaction in kidney stone disease. J Am Soc Nephrol 5: S37
25. Verkoelen CF, Romijn JC, Boeve ER, Schroder FH (1996) Cell cultures as a model in the study of nephrolithiasis. Ital J Mineral Electrolyte Metab 10: 57
26. Hammes MS, Lieske JC, Pawar S, Spargo BH, Toback FG (1995) Calcium oxalate monohydrate crystals stimulate gene expression in renal epithelial cells. Kidney Int 48: 501
27. Fritzsch G, Rumrich G, Ullrich KJ (1989) Anion transport through the contraluminal cell membrane of renal proximal tubule. the influence of hydrophobicity and molecular charge distribution on the inhibitory activity of organic anions. Biochem Biophys Acta 978: 249
28. Kuo SM, Aronson PS (1988) Oxalate transport via the sulfate/HCO_3 exchanger in rabbit renal basolateral membrane vesicles. J Biol Chem 263: 9710
29. Koul H, Ebisuno S, Renzulli L, Yanagawa M, Menon M, Scheid C (1994) Polarized distribution of oxalate transport systems in LLC-PK1 cells, a line of renal epithelial cells. Am J Physiol 266: F266
30. Koul H, Kennington L, Honeyman T, Jonassen J, Menon M, Scheid C (1996) Activation of c-myc gene mediates the mitogenic effects of oxalate in LLC-PK_1 cells, a line of renal epithelial cells. Kidney Int 50: 1525
31. Scheid C, Koul H, Hill WAG, Luber-Narod J, Jonassen J, Honeyman T, Kennington L, Kohli R, Hodapp J, Ayvazian P, Menon M (1996) Oxalate toxicity in LLC-PK_1 cells, a line of renal epithelial cells. J Urol 155: 1112
32. Yoshimura A, Taira T, Ideura T (1996) Expression of apoptosis-related molecules in acute renal injury. Exp Nephrol 4: 15
33. Kim J, Cha J, Tisher TC, Madsen KM (1996) Role of apoptotic and nonapoptotic cell death in the removal of intercalated cells from developing rat kidney. Am J Physiol 270: F535
34. Lieberthal W, Triaca V, Levine JS (1996) Mechanisms of death induced by cisplatin in proximal tubular epithelial cells: apoptosis vs necrosis. Am J Physiol 270: F700
35. Lieberthal W, Levine JS (1996) Mechanisms of apoptosis and its potential role in renal tubular cell injury. Am J Physiol 271: F477
36. Bigelow MW, Wiessner JH, Kleinman JG, Mandel NS (1996) Calcium oxalate crystal membrane interactions, dependence on membrane lipid composition. J Urol 155: 1094
37. Khan SR(1997) Interactions between stone forming calcific crystals and macromolecules. Urol Int 59: 59
38. Wiessner JH, Hasegawa AT, Hung LY, Mandel GS, Mandel NS (2001) Mechanisms of calcium oxalate crystal attachment to injured renal collecting duct cells. Kidney Int 59: 637
39. Nishio S, Ide M, Yokoyama M, Iwata H, Takeuchi M (1996) Production of heparan sulfate in rat renal tubules in the process of calcium oxalate microlith formation, In: Pak CYC, Resnick MI, Preminger GM (eds) Urolithiasis. Millet, Dallas, p 32
40. Khan SR (1997) Interactions between stone-forming calcific crystals and macromolecules. Urol Int 59: 59

41. Oltvani ZN, Milliman CL, Korsmeyer SJ (1993) Bcl-2heteromerizes in vivo with a conserved homolog, Bax, that accelerates programmed cell death. Cell 74: 609
42. Clarke AR, Purdie, CA, Harrison DJ, Morris RG, Bird CC, Hooper ML, Wyllie AH (1993) Thymocyte apoptosis induced by p53-dependent and independent pathways. Nature 362: 849
43. Miyashita T, Reed JC (1995) Tumor suppressor p53 is a direct transcription activator of the human Bax gene. Cell 80: 293
44. Hermeking H, Eick D (1994) Mediation of c-myc-induced apoptosis by p53. Science 265: 2091
45. Thulasi R, Harbour DV, Thompson EB (1993) Suppression of c-myc is a critical step in glucocorticoid-induced human leukemic cell lysis. J Biol Chem 268: 18306
46. Hueber AO, Zornig M, Lyon D, Suda T, Nagata S, Evan GI(1997) Requirement for the CD95 receptor-ligand pathway in c-myc-induced apoptosis. Science 278: 1305
47. Ortiz A, Neilson EG (1993) Apoptosis-related Fas mRNA is expressed by renal cells and increased in renal damage. J Am Soc Nephrol 4: 496
48. Nagata S, Golstein P(1995) The fas death factor. Science 267: 1449
49. Enari M, Hug H, Nagata S (1995) Involvement of an ice-like protease in fas-mediated apoptosis. Nature 375: 78
50. Tewari M, Dixit VM (1995) Fas- and tumor necrosis factor-induced apoptosis is inhibited by the poxvirus crmA gene product. J Biol Chem 270: 3255